

# High-Temperature Heterogeneous Reaction Kinetics of Tungsten Oxidation by CO<sub>2</sub>, CO, and O<sub>2</sub>

Justin L. Sabourin\* and Richard A. Yetter†

*Pennsylvania State University, University Park, Pennsylvania 16802*

DOI: 10.2514/1.38123

**The high-temperature heterogeneous reaction rates of bulk tungsten are studied using thermogravimetric analysis in oxygen (O<sub>2</sub>), as well as carbon dioxide (CO<sub>2</sub>) and carbon monoxide (CO) atmospheres. Isothermal reaction rates were determined at temperatures ranging from 1300 to 1700°C. Constant system pressures of 1 atm were employed; however, O<sub>2</sub> and CO<sub>2</sub> partial pressures ranged from 0.152 to 3.8 torr and 7.6 to 64.6 torr, respectively. Using Arrhenius reaction rate kinetics, activation energies of the W–O<sub>2</sub> and W–CO<sub>2</sub> reactions were found to be 23.5 and 64 kcal/mol, whereas pressure exponents were determined to be 0.89 and 0.6, respectively. Oxidation rates were higher for O<sub>2</sub> than CO<sub>2</sub> under constant partial pressure conditions. Increasing CO concentration in the presence of constant CO<sub>2</sub> partial pressure was found to reduce reaction rates significantly, emphasizing the impact gas mixtures may have on heterogeneous reaction rates. The results imply chemical erosion rates of nozzles may be altered significantly by small perturbations in propellant formulations, and O<sub>2</sub> may play a nonnegligible role, even in very small quantities present in rocket motors.**

## I. Introduction

TO INCREASE the performance of future rocket motor systems, chamber pressures and temperatures will be increased well beyond current operating conditions, introducing new challenges to scientists and engineers. One of these challenges is to improve nozzle performance by reducing erosion, particularly chemical erosion (corrosion). This has led to a large increase in research over the last few years, aimed at improving the understanding of nozzle erosion so that new engineering concepts may be introduced relating to both motor and propellant design [1–5].

The bulk oxidation of refractory materials such as tungsten (W), which is a primary constituent of current and future rocket nozzle surfaces, plays an important role in the overall erosion mechanism. Therefore, a fundamental understanding of the chemical processes occurring at and below the metal surface, as well as within the nozzle fluid boundary layer, is important to the development of forthcoming nozzles which will operate at increased temperatures and pressures from today's standards. The anticipated increase in operating conditions of future rocket motors increases both physical and chemical strain on all rocket components, particularly nozzle throats, where elevated heat transfer rates may increase erosion rates, causing performance reductions and possible failure.

Rocket nozzle recession may be caused by various phenomena or mechanisms ranging from vaporization of the nozzle material, to structural failure caused by particle impact, applied pressure, or thermal stresses [6–9]. The primary erosion mechanisms of refractory metals such as tungsten, which have high melting temperatures (~3680 K for W), often stem from heterogeneous reactions at the nozzle surface forming various metal containing compounds. Many of these surface reaction product compounds exhibit vaporization and/or melting temperatures much less than that of refractory nozzle material and combustion flame temperatures. Moreover, nonadherent solid compounds may be formed at the metal surface. In these cases the compounds may be removed from the

nozzle surface nearly as fast as they are formed, either by the shear forces created by high pressure gas flow, or vaporization of the compounds into the gas stream. The overall effect of these chemical mechanisms is the removal of bulk nozzle material and the expansion of the nozzle throat area, reducing overall rocket performance.

To model and understand rocket nozzle erosion, surface reaction characterization becomes a very important piece to the overall process. The majority of the reactions occurring at the surface of tungsten nozzles are oxidation reactions, which occur rapidly at high temperatures. The high-speed flows also reduce the nozzle surface boundary layers, reducing the distance which the oxidizing combustion products must be transported to adsorb and react with the nozzle material. Particularly with solid rocket motors, fuel rich conditions exist and the primary oxidizing species of nozzles are CO<sub>2</sub>, H<sub>2</sub>O, CO, OH, O, and NO. Determination of fundamental reaction kinetics of basic reactions including the oxidizers above is the first step in building a reaction mechanism. Although heterogeneous reaction kinetics of individual species are often affected by the presence of other species, understanding the individual kinetics provides an elementary framework to build more complex models. To date there has been several studies of gas–solid surface reaction kinetics of bulk tungsten at high temperature, with most involving the reaction of tungsten and molecular oxygen (O<sub>2</sub>) [10–15]. Less work has been done with other compounds such as CO<sub>2</sub> [16,17], H<sub>2</sub>O [18–21], O [22], or nitrogen containing compounds [23], and even less has looked into how mixtures of these compounds may affect overall reaction rates [16,24,25]. Most of this work presents a phenomenological perspective of oxidation rates, which may not be adequately applied to modeling and prediction of kinetic rates. This limited pool of available kinetic data has restricted development of new models used to predict nozzle erosion rates [5].

Most high-temperature oxidation reactions occur fairly rapidly, consuming reactants and creating a concentration gradient between the surrounding gas and the surface. If the diffusion time scale of the reactant to the metal surface is not at least as fast as the chemical reaction time scale, apparent reaction kinetics may be considerably different from the true chemical reaction kinetics [26]. In static reactor experiments, which are used in most of the previous studies of high-temperature oxidation kinetics, apparent rates, activation energies, and reaction orders are often different from true values unless the diffusional limitation is recognized and treated accordingly.

In the case of tungsten oxidation at high temperatures, the oxides are vaporized as fast as they are formed, and the rate of oxidation follows a linear rate law, which increases exponentially with

Received 17 April 2008; revision received 23 October 2008; accepted for publication 23 October 2008. Copyright © 2008 by the American Institute of Aeronautics and Astronautics, Inc. All rights reserved. Copies of this paper may be made for personal or internal use, on condition that the copier pay the \$10.00 per-copy fee to the Copyright Clearance Center, Inc., 222 Rosewood Drive, Danvers, MA 01923; include the code 0748-4658/09 \$10.00 in correspondence with the CCC.

\*Ph.D. Candidate, Department of Mechanical and Nuclear Engineering, 14 Research Building East.

†Professor of Mechanical Engineering, 111 Research Building East. Member AIAA.

temperature. Because nonadherent oxides are formed, the oxidation rates may be kinetically limited by surface collision rates, surface species dissociation or migration, and/or surface desorption processes. As the concentration of oxidizing molecules is increased, so are the rates of collision, increasing the overall oxidation rate until at very high concentrations the surface becomes saturated with oxidizing molecules and the rate becomes independent of concentration [12]. At lower pressures, the linear rate law is a function of both pressure and temperature, as described by the Arrhenius rate equation:

$$k_i(T, P) = A_i \cdot \exp(-E_i/Ru \cdot T_s) \cdot P_i^{n_i} \quad (1)$$

where  $k$  (units of  $\text{W} \cdot \text{cm}^{-2} \cdot \text{s}^{-1}$ ) is the reaction rate,  $A$  is the preexponential factor,  $E$  is the activation energy,  $Ru$  is the universal gas constant,  $T_s$  is the W surface temperature,  $P$  is the oxidizer partial pressure,  $n$  is a pressure exponent, and the subscript  $i$  refers to the oxidizing species (i.e.,  $\text{O}_2$  or  $\text{CO}_2$ ).

This paper presents results on the high-temperature heterogeneous reaction kinetics of tungsten in the presence of  $\text{O}_2$ ,  $\text{CO}_2$ , and  $\text{CO}$ . Reactions involving  $\text{CO}_2$  and  $\text{CO}$  have been studied previously [16,24]; however, the work by Walsh et al. [16] is the only study in which rates have been characterized as a function of temperature and pressure and presented quantitatively in mathematical form. Because  $\text{CO}_2$  and  $\text{CO}$  are primary product species in solid propellant rocket motor nozzles, a detailed understanding of the heterogeneous reaction kinetics is required to improve modeling capabilities and accuracy. The oxidation rates of W by  $\text{O}_2$  are studied and presented as well. Although  $\text{O}_2$  is not generally a primary species in rocket exhausts, it provides a simple system for experimental validation, while increasing the knowledge base of fundamental high-temperature refractory metal oxidation. The implications of these results are discussed in relation to the corrosion of rocket nozzles as well.

## II. Experimental Approach

The oxidation kinetics of bulk tungsten were obtained under isothermal conditions by measuring the weight change over time using a thermogravimetric analyzer (TGA) developed at The Pennsylvania State University. The primary components of the TGA are a Cahn D-101 digital recording balance, capable of measuring changes in mass as low as  $1 \mu\text{g}$ , an Applied Test Systems vertical tube furnace, which has a maximum temperature of  $1700^\circ\text{C}$ , and several Teledyne Hastings mass flow controllers (200 series) to regulate the flow of each gas to within  $\pm 1\%$ . A schematic of the TGA system is shown in Fig. 1. Test samples of tungsten foil were cut from 99.95% W foil obtained from Goodfellow (W 000315). Originally,

25- $\mu\text{m}$ -thick foils were used but were too thin, reducing the number of test runs which could be completed before appreciable changes in surface areas occurred. Subsequent tests have used 200- $\mu\text{m}$ -thick foils, which have shown to erode fairly uniformly, maintaining an overall rectangular shape during testing. Dimensions are, however, slightly reduced during testing and slight tapers have been found at the leading edge, due to flow stagnation and boundary-layer development. These small changes in sample dimensions were estimated during testing using the mass loss of tungsten from each test run. The maximum change in sample surface area was found to be 15%, spread over 29 runs; therefore, each run was assumed to take place at a constant surface area. Although samples of various dimensions have been used, varying from 1.5 to 2.8  $\text{cm}^2$ , most testing was completed using  $8.35 \times 16.25 \text{ mm}$  foil samples; testing indicated reaction rates ( $\text{g}/\text{cm}^2 \cdot \text{s}$ ) of various sample sizes were within experimental uncertainties of each other [27]. Because of difficulties in shearing the 200  $\mu\text{m}$  foils, electrical discharge machining (EDM) was used to cut the samples. This method not only allowed for very smooth cuts to be made, but enabled precise dimensions to be held.

The high temperatures, oxidative atmospheres, and time scales of testing restricted the pool of materials which could be used within the system. To control the atmosphere within the furnace, a high purity alumina reaction tube (0.875 in outer diameter, 0.625 in inner diameter) was used. The tube was sealed directly to the balance and gas connections using O-rings to eliminate leaks in the reaction system. The tungsten samples were suspended from the microbalance into the furnace by sapphire suspensions produced by Photran, LLC (Poway, California). The sapphire suspensions were required because of their high-temperature performance, ductility, strength, and chemical inertness in oxidative atmospheres. Small holes ( $\sim 1 \text{ mm}$ ) were cut into the samples using a carbide bit so they could be hung from the suspensions. To minimize the reaction of tungsten during system heating, pre- and postruns, ultrahigh purity inert gases were used (99.999%). During heating to the desired test temperature hydrogen ( $\text{H}_2$ ) was flowed through the TGA to clean the metal surface of oxides or other impurities and limit oxidation by trace impurities in the gas stream. All tests were conducted using helium (He) as the carrier gas, which kept oxidative gas concentrations low and protected the balance from chemical attack. Further purification was accomplished by running the  $\text{H}_2$  and He gases through copper coils submerged in liquid nitrogen to condense  $\text{H}_2\text{O}$  and  $\text{O}_2$ , removing them from the gas flow. The system temperature adjacent to the tungsten sample was monitored using a type-C (W-Re) thermocouple, which has an accuracy of  $\pm 1.0\%$ . The thermocouple was protected from chemical attack by a high purity alumina tubewell.

Once the desired system temperature was reached, the system was allowed to stabilize for a minimum of 15 min before testing. During all tests, system flow rates, temperature, mass, and time were recorded using a National Instruments data acquisition card (NIPCI-6014) used in cooperation with a LabVIEW interface program. LabVIEW also allowed for simultaneous control of the flow rates using up to four different mass flow controllers (MFCs) through the MFC power supply (Teledyne Hastings THPS-400). All test information was recorded at a sampling rate of 1 Hz, which was the maximum sampling rate set by the communication with the Cahn balance. Tests lasted as little as 20 s in duration to more than 3 min, depending on the oxidizer type, concentration, and temperature. The reaction rates were determined by the slope of the mass loss curve over time ( $dm/dt$ ); in most cases a least-squares fit of the data produced  $R^2$  values greater than 0.999. No cases were found which did not produce a linear mass loss curve.

Diffusion limited reactions were eliminated or reduced to negligible levels in the TGA by using high volume flows. To determine the required flow rates to create kinetically limited conditions, temperature and oxidizer concentration were kept constant while increasing flow rate. As flow rates approach kinetically limited conditions, reaction rates (i.e., W mass loss rate) become independent of flow rate. Because of high reaction rates between W and  $\text{O}_2$ , diffusion limited reactions were found at the

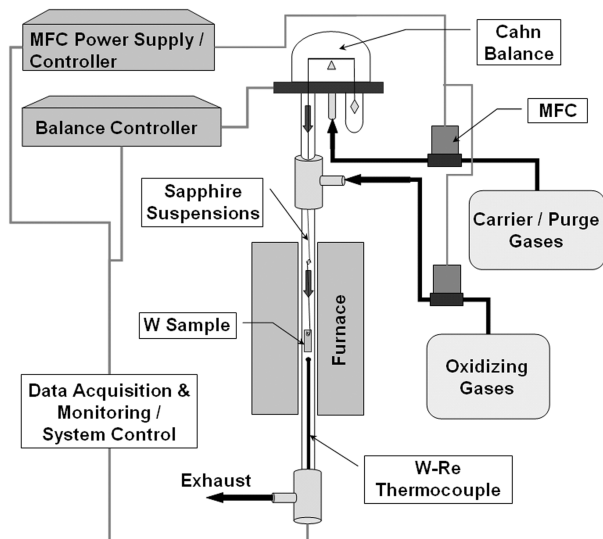


Fig. 1 Schematic of TGA used for determination of heterogeneous reaction kinetics.

maximum system temperature and flow rate, reducing the temperature range of the applicable kinetic data. In the case of the W and CO<sub>2</sub> reaction, kinetically limited reactions were found over the entire temperature range using a system flow rate of 7 SLPM (standard liters per minute,  $P_{\text{std}} = 760$  torr,  $T_{\text{std}} = 0^\circ\text{C}$ ). Examples of raw data and the testing used to determine kinetically controlled conditions are presented elsewhere [27].

### III. Results and Discussion

The results of these oxidation studies are presented in the following sections for varying temperatures and partial pressures of the subject species, followed by a corollary discussion of the effects of nozzle erosion rates under rocket motor conditions. Results of oxidation kinetics are compared and contrasted with previous literature as well.

#### A. Oxidation Kinetics in Presence of O<sub>2</sub>

The oxidation rate of bulk tungsten in the presence of molecular oxygen was studied at partial pressures between 0.152 and 3.8 torr (0.02–0.51 kPa or 0.02–0.5%). The overall oxidation rates were found to be fast and therefore, at the highest temperatures considered, diffusion limited reactions were found, as indicated by the onset of what appears to be temperature independent or inversely dependent reactions at high temperatures in Fig. 2. A maximum reactor flow rate of 17 SLPM was used; larger flow rates were not used due to concerns of reducing the sample temperature. To determine the activation energy of the tungsten and oxygen heterogeneous reaction ( $E_{\text{O}_2}$ ), the highest temperatures were neglected ( $>1875$  K) determining  $E_{\text{O}_2}$  to be 22.6 kcal/mol of tungsten on average, with a standard deviation of 1.4. This activation energy is within the range of values found by previous researchers (14.3–48 kcal/mol) as shown in Table 1. However, many of these studies involved either lower temperatures or static flow conditions. The work by Walsh et al. [15] is the only study in which high flows were used to remove diffusion limited reactions at very high temperatures, determining the activation energy to be 23 kcal/mol, nearly the exact value determined in this study.

The oxygen pressure dependence on the reaction rate was determined from the slope of constant temperature data when plotting  $\ln(k_{\text{O}_2})$  versus  $\ln(P_{\text{O}_2})$ , yielding a pressure exponent ( $n_{\text{O}_2}$ ) of 0.90 with a standard deviation of 0.01. Tests determining this pressure exponent were conducted in the same session using the same sample, thus minimizing errors. Oxygen partial pressures used ranged from 0.152 to 3.8 torr during these tests. The pressure exponent of near unity indicates a reaction rate nearly proportional to the collision frequency of oxygen molecules with the bulk surface, and is not rate limited by the desorption of volatile oxides, or O<sub>2</sub>

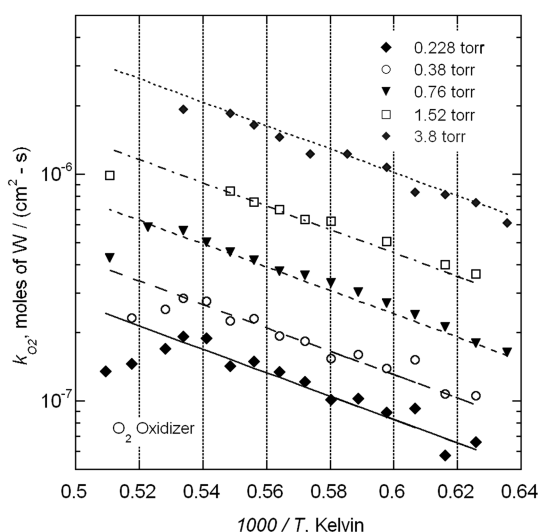


Fig. 2 Rates of tungsten consumption by O<sub>2</sub> [lines from Eq. (2)].

dissociation at the surface. Other researchers have found pressure exponents as high as 1.35 [28] and as low as 0.55 [13]. Much of the previous literature does not report a pressure exponent.

Using the pressure dependence of the W–O<sub>2</sub> oxidation reaction derived previously, the Arrhenius reaction rate preexponential factor ( $A_{\text{O}_2}$ ) was estimated by manipulation of Eq. (1), plotting the  $\ln(k_{\text{O}_2}/P_{\text{O}_2}^{n_{\text{O}_2}})$  vs  $1/T$ , where  $A_{\text{O}_2}$  is the y-axis intercept. These results provide an initial estimate of an appropriate analytical model of tungsten oxidation by O<sub>2</sub>; however the model was refined within the range of uncertainty, increasing accuracy of predictions with the majority of data. This model is shown in Eq. (2). The oxidation rates predicted by this correlation are shown in Fig. 2, where the molecular weight of tungsten is 183.84 g/mol. The derived Arrhenius rate function predicts measured rates within acceptable limits of error, as most of the data is within  $\pm 10\%$ , and all is within  $\pm 20\%$  ( $1572 < T < 1875$  K):

$$k_{\text{O}_2} = A_{\text{O}_2} \cdot \exp\left[\frac{-E_{\text{O}_2}}{Ru \cdot T_s}\right] \cdot [P_{\text{O}_2}]^{n_{\text{O}_2}} \\ = 3.8 \times 10^{-4} \frac{\text{mol of W}}{\text{cm}^2 \cdot \text{s} \cdot \text{torr}^{0.89}} \cdot \exp\left[\frac{-23.5 \frac{\text{kcal}}{\text{mol}}}{Ru \cdot T_s}\right] \cdot [P_{\text{O}_2}]^{0.89} \quad (2)$$

#### B. Oxidation Kinetics in Presence of CO<sub>2</sub> and CO

The oxidation rate of bulk tungsten in the presence of carbon dioxide was studied at partial pressures between 7.6 and 64.6 torr (1.01–8.61 kPa or 1.0–8.5%). As expected, based on previous literature, no measurable tungsten oxidation was found with carbon monoxide alone. The overall oxidation rates were also found to be slower than found with O<sub>2</sub>, and therefore overall reactor flow rates of 7 SLPM were found to produce kinetically limited reaction rates at all temperatures considered. Oxidation rate results at various CO<sub>2</sub> partial pressures are shown in Figs. 3 and 4. Fitting the results of these figures to the Arrhenius expression [Eq. (1)], the activation energy ( $E_{\text{CO}_2}$ ) of the W–CO<sub>2</sub> reaction is determined to be on average 63.6 kcal/mol of reacted tungsten, with a standard deviation of 2.6 kcal/mol. This activation energy is nearly triple that of the O<sub>2</sub> oxidation reaction, indicating a much greater energy barrier in forming a gas phase tungsten oxide from CO<sub>2</sub>. This activation energy is lower than 79 kcal/mol, which is the value found by Walsh et al. [16]. A summary of the previous reaction kinetics studies of W and CO<sub>2</sub> is shown in Table 2. The work by Harvey [17] involves solely diffusion limited reactions.

The carbon dioxide pressure dependence on the oxidation rate was determined using the same procedure as with the W–O<sub>2</sub> system, determining the pressure exponent ( $n_{\text{CO}_2}$ ) to be 0.60 with a standard deviation of 0.03. The pressure dependence, which is much less than unity, indicates a desorption or dissociation limited reaction. The limiting dissociation process could be due to the dissociative adsorption of CO<sub>2</sub> into CO and O. A limiting desorption process may be due to formed CO, or a volatile tungsten oxide. Detailed modeling is required to resolve the dominant or limiting reaction routes.

Using the pressure dependence of the W–CO<sub>2</sub> oxidation reaction, the Arrhenius reaction preexponential factor ( $A_{\text{CO}_2}$ ) was estimated using the same graphical plotting procedure discussed previously. As with the previous system, these results provided an initial estimate of an appropriate analytical model of tungsten oxidation by CO<sub>2</sub>. With refinement, an empirically derived analytical kinetic model for tungsten oxidation by CO<sub>2</sub> was developed, shown in Eq. (3). Most of the data of Figs. 3 and 4 lay within  $\pm 15\%$  of the Arrhenius fit, and nearly all data were within  $\pm 20\%$ :

$$k_{\text{CO}_2} = A_{\text{CO}_2} \cdot \exp\left[\frac{-E_{\text{CO}_2}}{Ru \cdot T_s}\right] \cdot [P_{\text{CO}_2}]^{n_{\text{CO}_2}} \\ = 0.285 \frac{\text{mol of W}}{\text{cm}^2 \cdot \text{s} \cdot \text{torr}^{0.67}} \cdot \exp\left[\frac{-64 \frac{\text{kcal}}{\text{mol}}}{Ru \cdot T_s}\right] \cdot [P_{\text{CO}_2}]^{0.6} \quad (3)$$

Although carbon monoxide was found to produce no measurable oxidation rates using the TGA, CO was found to affect oxidation

**Table 1** Summary of previous W–O<sub>2</sub> high-temperature kinetics studies

| Authors, yr                    | System pressure, torr       | System Temp., °C | Partial O <sub>2</sub> pressure, torr         | Experimental method  | <i>E</i> , kcal/mol | Pressure exponent, <i>n</i> | Author comments/<br>conclusions   |
|--------------------------------|-----------------------------|------------------|---|--|---------------------|-----------------------------|---|
| Baur et al., 1956 [10]         | (assumed = $P_{O_2}$ )      | 1107–1627        | 1034–25,840                                   | TGA ( $\Delta m/\Delta t$ ), static flow furnace   | 48                  | —                           | WO <sub>2</sub> and WO <sub>3</sub> products found  |
| Gulbransen & Andrew, 1960 [11] | <760 (assumed = $P_{O_2}$ ) | 500–1300         | 1–76  | TGA ( $\Delta m/\Delta t$ ), static flow furnace   | 32.5                | —                           | Rate limited by WO <sub>3</sub> volatility, diffusion of O <sub>2</sub> and W <sub>3</sub> O <sub>9</sub> products, mass loss @ $T > 1200^\circ\text{C}$                                  |
| Perkins & Crooks, 1961 [12]    | 1–40                        | 1300–3000        | 0.21–8.4 (assuming 21% O <sub>2</sub> in air) | Surface recession ( $\Delta x/\Delta t$ ), static flow, resistively heated sample                            | 31.5 (1300–1750°C)  | 0.62 (1300–1750°C)          | Above 1750°C the reverse reaction rate (dissociation of WO <sub>3</sub> on surface) becomes important and decreases reaction rate   |
| Gulbransen et al., 1964 [14]   | (assumed = $P_{O_2}$ )      | 1150–1615        | 2–100   | TGA ( $\Delta m/\Delta t$ ), static flow furnace   | 14.3                | 1.1                         | ~13% of O <sub>2</sub> molecules colliding w/surface react (i.e. sticking factor = 0.13)  |
| Bartlett, 1964 [13]            | <760 (assumed = $P_{O_2}$ ) | 1320–3170        | 0.00076–760                                   | Surface recession ( $\Delta x/\Delta t$ ), resistively heated sample   | 42                  | 0.55–0.8                    | Above 2000°C reaction probabilities were 0.06 @ all pressures and reaction rate was independent of $T$ , multilayer kinetic process suggested forming WO <sub>2</sub> and WO <sub>3</sub> |
| Walsh et al., 1967 [15]        | 2–11.1 (static)             | 1727–3027        | 0.11–11.5 (stagnation)                        | Surface recession [ $\Delta(x_f - x_i)/\Delta t$ ], high velocity jet impingement, inductively heated sample | 23                  | —                           | Diffusion limited rates found at highest temperatures   |
| Harvey, 1973 [28]              | 600                         | 2177–2927        | 0.012–0.09                                    | Mass change [ $\Delta(m_f - m_i)/\Delta t$ ], static flow, resistively heated sample                         | —                   | 1.10–1.35                   | Reaction rates at constant O <sub>2</sub> partial pressure decreased w/ increasing $T$ in this diffusion limited system   |

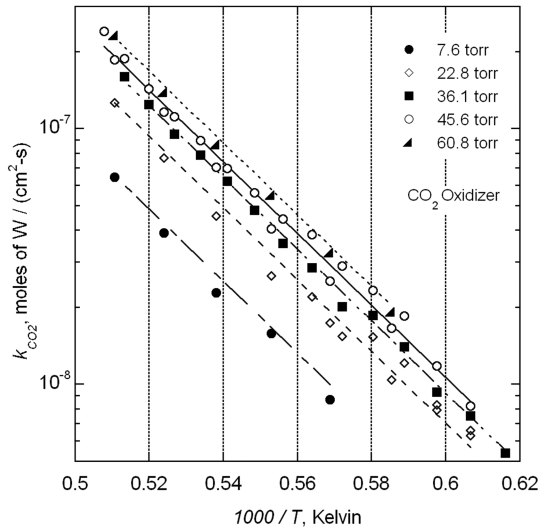


Fig. 3 Rates of tungsten consumption by CO<sub>2</sub> [lines from Eq. (3)].

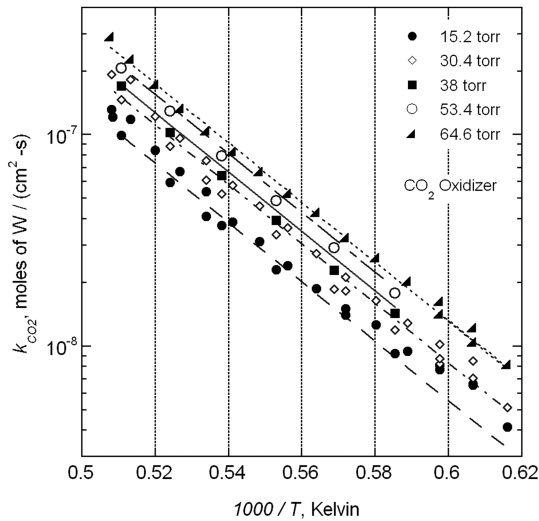


Fig. 4 Rates of tungsten consumption by CO<sub>2</sub> [lines from Eq. (3)].

rates of CO<sub>2</sub> considerably. This effect was observed previously by other researchers [16,24], however Walsh et al. [16] have been the only research group to quantify the effect of CO on the oxidation rates of CO<sub>2</sub> as a function of temperature and pressure. The effects of the CO addition on CO<sub>2</sub> oxidation rates were determined at a constant partial pressure of 34.2 torr, and CO to CO<sub>2</sub> ratios up to 4

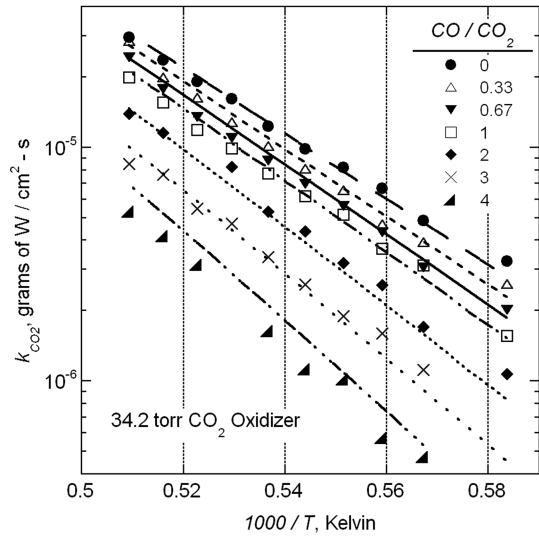


Fig. 5 Effect of CO on the CO<sub>2</sub> oxidation rates of tungsten [lines from Eq. (4)].

(Fig. 5). The plot shows that although the CO does not cause the consumption of bulk tungsten, it does significantly affect the oxidation rates involving CO<sub>2</sub>. The activation energy of the W–CO<sub>2</sub> reaction is affected by the addition of CO as well. Curve fitting of the data in Fig. 5 illustrated activation energies of 59.1, 63.5, 65.7, 63.3, 70.7, 71.1, and 85.1 kcal/mol at ratios of 0, 0.33, 0.67, 1, 2, 3, and 4, respectively, indicating stronger temperature dependence when a large amount of CO is present. Up to a ratio of unity, activation energies are within experimental error of each other, signifying that the CO does not change the limiting reaction steps in the overall mechanism. However, at high ratios it seems clear that CO alters the limiting reaction steps.

To better quantify the effect of CO on the rates of oxidation involving CO<sub>2</sub> and W, Fig. 6 was created and an empirical correlation was applied to the data [Eq. (4)]. The results indicate that reaction rates are significantly affected by CO, even at ratios less than 0.33. These figures illustrate a temperature dependent pattern relating to the CO addition. As a caveat, this correlation is a greatly simplified approach for describing the presence of CO on the overall reaction rates and therefore contains a great deal of empiricism.

The abilities of the empirical correlations to predict the kinetic reaction rates of tungsten oxidation are shown in Figs. 3–5 in the form of solid and dashed lines. The correlations perform well over the range of conditions in this study. Walsh et al. developed a similar equation, however; in their correlation the effect of CO is magnified with increasing temperature [see Eq. (5)] [16]. Using Eq. (5), the experimentally derived reaction rates of this study are under-predicted. However, the greater activation energy and pressure

Table 2 Summary of previous W–CO<sub>2</sub> high-temperature kinetics studies

| Authors, yr             | System pressure, torr | System temp., °C | Partial CO <sub>2</sub> pressure, torr | Experimental method  | E, kcal/mol | Pressure exponent, n | Author comments/conclusions  |
|-------------------------|-----------------------|------------------|--|--|-------------|----------------------|--|
| Walsh et al., 1967 [16] | 300 (static)          | 1927–3027        | 20–337 (stagnation)                    | Surface recession [Δ(x <sub>f</sub> – x <sub>i</sub> )/Δt], high velocity jet impingement, inductively heated sample | 79          | 0.88                 | Diffusion limited rates found @ high T (>2377°C), small CO additions showed depressed rates, overall rates much less than O <sub>2</sub> |
| Harvey, 1974 [17]       | 600                   | 2177–2727        | 0.0162–0.097                           | Mass change [Δ(m <sub>f</sub> – m <sub>i</sub> )/Δt], static flow, resistively heated sample                         | —           | 0.78–1.18            | Diffusion limited rates found throughout   |

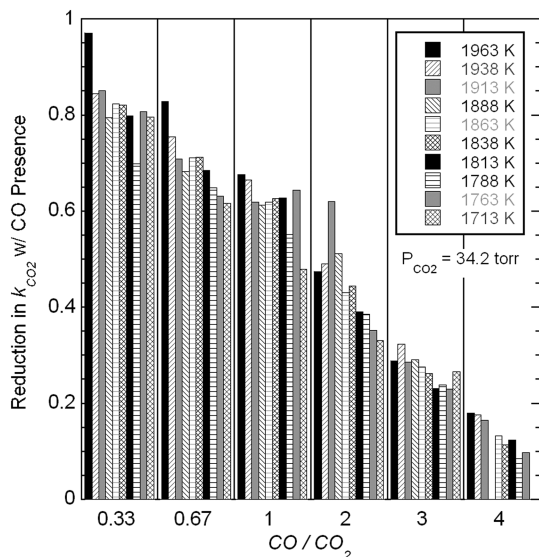


Fig. 6 Reduction in tungsten oxidation rate by CO<sub>2</sub> as function of CO:CO<sub>2</sub> ratio.

dependence causes Eq. (4) to underpredict the experimental data presented by Walsh et al. If the correlation to correct for CO and CO<sub>2</sub> mixtures developed by Walsh et al. is applied to Eq. (3), the reaction rates found in this study are overpredicted, as the calculated results indicate a CO<sub>2</sub> reaction rate reduction of less than 28% at the highest temperature (i.e., 1973 K) and CO concentration (i.e., 4 · CO:CO<sub>2</sub>) studied, compared to 77% in this study. In addition to studying two different temperature ranges, two significantly different experimental apparatuses were used in these studies. Walsh et al. used a stagnation flow reactor, where an inductively heated sample was oxidized with a stagnating flow of a known reactive mixture. The reactive mixture is applied for a given period of time and the sample recession is recorded by measuring pre- and post-test conditions. Additionally, total system pressures in the tests by Walsh et al. were less than 1 atm:

$$k_{\text{CO}_2/\text{CO}} = A_{\text{CO}_2} \cdot \exp\left[\frac{-E_{\text{CO}_2}}{R_u \cdot T_s}\right] \cdot [P_{\text{CO}_2}]^{n_{\text{CO}_2}} \cdot \exp\left[-(2.194 \times 10^{11} \cdot T^{-3.574}) \frac{P_{\text{CO}}}{P_{\text{CO}_2}}\right] \quad (4)$$

$$k_{\text{CO}_2/\text{CO}}(\text{Walsh et al.}) = 2.19 \cdot \exp\left[\frac{-79 \text{ kcal/mol}}{R_u \cdot T_s}\right] \cdot [P_{\text{CO}_2}]^{0.88} \left[1 - 0.547(P_{\text{CO}}/P_{\text{CO}_2}^{0.5})^{0.88} \cdot \exp\left[\frac{-14.7 \text{ kcal/mol}}{R_u \cdot T_s}\right]\right] \quad (5)$$

The reduction in tungsten oxidation rates by CO<sub>2</sub> with the introduction of CO may be caused by several mechanisms. The first is a function of the experimental conditions. At very high temperature, CO<sub>2</sub> will dissociate into CO, O, and O<sub>2</sub>. The addition of CO into a mixture of CO<sub>2</sub> will reduce the levels of dissociation at equilibrium. Using CHEMKIN 4.0 [29] the dissociation kinetics were modeled to determine how fast CO<sub>2</sub> dissociates under experimental conditions. The results showed that CO<sub>2</sub> will indeed dissociate into O<sub>2</sub> and O, which would increase reaction rates found using the TGA. At the highest temperatures considered, equilibrium concentrations of O<sub>2</sub> and O would cause severe increases in oxidation rates. However, negligible dissociation occurs at temperatures below 1400 K [30] and kinetics indicate that equilibrium conditions cannot be met given the time interval for dissociation of the CO<sub>2</sub> within the furnace before reaching the test sample. Time intervals of 50–150 ms have been estimated, given a

constant flow rate (7 SLPM) and varying reactor temperatures. In fact, calculations would indicate that changes in CO<sub>2</sub> reaction rates due to O<sub>2</sub> formation were less than 10% at 2000 K and 0.5% at 1750 K, with no CO addition. When there is twice as much CO in the system than CO<sub>2</sub>, changes are less than 0.5% at 2000 K. This variation is deemed acceptable given uncertainty in kinetic data and also verifies that the presence of CO directly affects the CO<sub>2</sub> oxidation rate. Additionally, results indicate a stronger CO influence at lower temperatures, supporting the fact that dissociation may not explain the reaction rate reduction. Moreover, if the dissociation of CO<sub>2</sub> were playing a significant role, reaction rates would increase dramatically at the highest temperatures studied when no CO is present. This result indicates that although dissociation of reactive gases should be considered in any experimental apparatus measuring reaction rates, it does not significantly affect CO<sub>2</sub> reaction rates found here, particularly at lower temperature, or in cases where CO is added to the gas mixture.

Another explanation for the reduction in reaction rates with CO addition are reductions in the net desorption rates of CO from the bulk surface, reducing available adsorption or dissociation sites for CO<sub>2</sub>, essentially reducing available surface area for reaction. Figure 7 helps explain this point, which illustrates several greatly simplified reactions. In reactions 1–5, as the CO partial pressure increases each reaction is driven increasingly in the direction of decreased partial pressure. This can either reduce reactive surface sites through CO adsorption (reactions 1 and 5), or decrease the net rate of CO<sub>2</sub> dissociation (i.e., decrease O-atom production, reactions 2–4); each in turn reduces rates of tungsten surface atom volatilization. Reactions 2 and 3 basically illustrate the same reaction; however, one creates a surface species tungsten dioxide, the other a gas phase species. Reactions 1 and 5 illustrate the nondissociative and dissociative CO adsorption processes, respectively. This shift in equilibrium has been used in the past as the primary explanation for reductions in the CO<sub>2</sub> oxidation rates with CO addition [24].

Based on the results of a recent theoretical study conducted by Chen et al. involving the adsorption of CO<sub>2</sub> and CO on a W(111) surface, the most likely scenario occurring is that dissociative adsorption (reactions 5 and 6) poisons the surface oxidation process [31]. The W–C bonding at the surface is calculated to be stronger than all other bonds at the surface (i.e. W–CO<sub>2</sub>, W–CO, W–O) and highly resistant to desorption or surface diffusion processes. Therefore, the additional carbon present at the surface due to dissociative adsorption of CO effectively reduces the available surface area for oxidation. The study of Chen et al. also estimated the kinetics of the adsorption processes. The dissociative adsorption rate of CO is predicted to be approximately 2 orders of magnitude slower than CO<sub>2</sub> adsorption; however, this does not account for desorption processes. Although the initial process of CO<sub>2</sub> adsorption may occur faster, equilibrium surface concentrations of carbon atoms at the surface should quickly be approached. The results of this study are supported by other studies involving CO adsorption on W(111) surfaces [32,33]. These studies indicate that CO oxidation is a self-poisoning process as the W–C bonding restricts dissociative

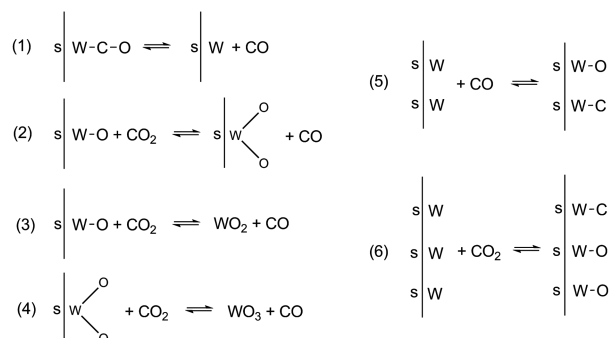


Fig. 7 Surface mechanisms containing CO which may affect oxidation rates.

adsorption of CO, thereby limiting the extent of oxidation and not allowing higher oxides to form which could dissociate, leading to corrosion or mass loss of the tungsten substrate. The kinetics also indicate a minimal activation energy for the adsorption reactions, which when compared to the global oxidation reaction energies found in the current study indicates a surface reaction or desorption limited reaction.

At this time there is some debate as to what the primary tungsten oxide desorption species is, although nearly all work points toward a mixture of  $\text{WO}_2$  and  $\text{WO}_3$  [34–36]. Mass-spectrometric studies of tungsten oxidation by  $\text{O}_2$  ranging in temperatures from 1400–3150 K indicate that at lower temperatures  $\text{WO}_3$  or one of its polymers are the primary desorption species, whereas at the highest temperatures  $\text{WO}_2$  is the dominant species. No previous studies have been located which determined if oxidizers such as  $\text{H}_2\text{O}$ , OH,  $\text{CO}_2$ , or NO affect the types of species vaporizing from an oxidizing tungsten surface. Although all studies involving this subject consider high-temperature conditions, evacuated environments are needed for spectroscopic measurements, and therefore none consider high pressure conditions such as present in the TGA, or a rocket motor. Experimental determination of desorption species under high temperature and pressure conditions is extremely difficult, as in situ methods are needed. In the past, researchers have relied on the chemical analysis of the solid oxides condensed in lower temperature regions, where chemical composition of tungsten oxides may differ significantly from that of the desorbing species. Most of the oxides formed on TGA tube walls and the thermocouple protection tube are a combination of purple, blue, and brown, indicating oxides of  $\text{WO}_{2.9}$  (blue) and  $\text{WO}_2$  (brown). As pressure increases, it may be assumed that the primary desorption species will shift toward the higher oxide,  $\text{WO}_3$ .

### C. Nozzle Corrosion Reactions and Rates

Molecular oxygen is generally viewed as playing a small and often negligible role in the oxidation rates of tungsten based rocket nozzles due to fuel rich conditions. Carbon dioxide and monoxide, however, are primary product species of solid rocket propellants which use hydrocarbon based fuels and binders. To explore the effects of these rates on nozzle erosion, a simple, nonaluminized ammonium perchlorate (AP) and hydroxyl-terminated polybutadiene (HTPB) propellant is considered. Using NASA Chemical Equilibrium with Applications (CEA) software [30], the equilibrium mole fraction of combustion product species is considered, as well as quasi-equilibrium mole fractions of nozzle boundary-layer species, assuming bulk tungsten as the primary component (Table 3). Using the equilibrium combustion product mole fractions, the kinetically limited throat recession rate may be estimated based on the  $\text{CO}_2$ , CO, and  $\text{O}_2$  pressures, and extrapolation of the previously developed equations to higher temperature ranges (see Fig. 8). Nozzle surface temperatures are estimated to be 400 K less than equilibrium. The results, considering each oxidizer individually, yield recession rates ( $r_c$ ) ranging from approximately 3–26  $\mu\text{m/s}$ , and illustrate the significant role CO plays in reducing the  $\text{CO}_2$  oxidation rates. Also

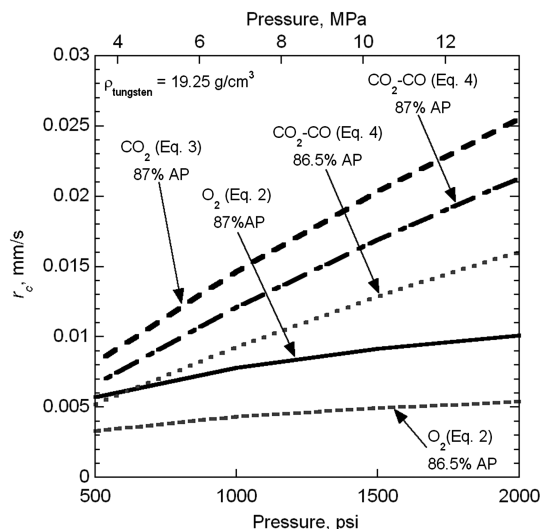


Fig. 8 Estimation of kinetically limited corrosion rates of a tungsten nozzle due to individual oxidizing species.

shown is the effect of changing propellant formulations or stoichiometry. A shift in 0.5% in mass of the propellant mixture causes rather significant changes in the estimated recession rates. The change in the  $\text{O}_2$  related recession rate is proportional to the change in  $\text{O}_2$  partial pressure in the product gas stream; however, the increased CO: $\text{CO}_2$  ratio due to increased HTPB concentration causes a nonproportional change in the  $\text{CO}_2$  related recession rate. These results would also indicate that even in minute quantities,  $\text{O}_2$  may create an appreciable amount of corrosion within a rocket motor due to high pressure conditions and may not be immediately neglected without consideration. It is also interesting to note that the calculated specific impulse of these two propellant formulations changes less than 0.1%.

Table 3 shows that the primary oxidizing species, in terms of overall partial pressures, are  $\text{H}_2\text{O}$ ,  $\text{CO}_2$ , and OH. Hydrogen chloride (HCl) is present in significant quantities as well, but has been shown to produce little to no erosion of bulk tungsten [18,24], although the presence of chlorine ( $\text{Cl}_2$ ) has been found to increase tungsten oxidation rates of  $\text{O}_2$ . Rosner and Allendorf [25] determined that when  $\text{Cl}_2$  is added to a constant  $\text{O}_2$  pressure mixture, ablation rates of tungsten are significantly increased, as the primary oxide product is shifted to  $\text{WO}_2\text{Cl}_2$  or some other tungsten oxychloride. Similar to the case of  $\text{CO}_2$  and CO, the addition of  $\text{H}_2$  to a constant pressure  $\text{H}_2\text{O}$  mixture has been found by Olcott and Batchelor [24] to reduce oxidation rates. These conclusions, in addition to the results of this study and Walsh et al. [16], all demonstrate that heterogeneous tungsten oxidation rates are significantly affected by gas mixture constituents and relative concentrations. Individual system kinetics may not be used to accurately predict reaction rates of multi-component systems using “additive” or other simplified techniques.

Table 3 Equilibrium combustion and boundary-layer species using a nonmetallized AP-HTPB propellant and tungsten nozzle

| 87% AP – 13% HTPB (mass)<br>$P = 1000 \text{ psi} = 6.89 \text{ MPa}$<br>$T_{\text{equil}} = 2946 \text{ K}$ |  | 86.5% AP – 13.5% HTPB (mass)<br>$P = 1000 \text{ psi} = 6.89 \text{ MPa}$<br>$T_{\text{equil}} = 2909 \text{ K}$ |  |
|--|--|--|--|
| Primary combustion species   | Primary boundary-layer species                     | Primary combustion species   | Primary boundary-layer species                     |
| $Y_{\text{H}_2\text{O}} = 0.395$   | $Y_{\text{W}(\text{cr})} = 0.320$                  | $Y_{\text{H}_2\text{O}} = 0.385$   | $Y_{\text{W}(\text{cr})} = 0.322$                  |
| $Y_{\text{HCl}} = 0.180$   | $Y_{\text{H}_2} = 0.155$                           | $Y_{\text{HCl}} = 0.178$   | $Y_{\text{H}_2} = 0.150$                           |
| $Y_{\text{CO}} = 0.135$  | $Y_{\text{H}_2\text{O}} = 0.152$                   | $Y_{\text{CO}} = 0.148$  | $Y_{\text{H}_2\text{O}} = 0.156$                   |
| $Y_{\text{CO}_2} = 0.104$  | $Y_{\text{CO}} = 0.145$                            | $Y_{\text{CO}_2} = 0.099$  | $Y_{\text{CO}} = 0.136$                            |
| $Y_{\text{N}_2} = 0.093$   | $Y_{\text{HCl}} = 0.081$                           | $Y_{\text{N}_2} = 0.092$   | $Y_{\text{HCl}} = 0.080$                           |
| $Y_{\text{H}_2} = 0.069$   | $Y_{\text{WO}_2(\text{OH})_2} = 0.032$             | $Y_{\text{H}_2} = 0.080$   | $Y_{\text{WO}_2(\text{OH})_2} = 0.036$             |
| $Y_{\text{Cl}} = 0.009$  | $Y_{\text{WO}_2\text{Cl}_2} = 0.023$               | $Y_{\text{Cl}} = 0.006$  | $Y_{\text{WO}_2\text{Cl}_2} = 0.025$               |
| $Y_{\text{OH}} = 0.008$  | $Y_{\text{CO}_2} = 0.019$                          | $Y_{\text{OH}} = 0.007$  | $Y_{\text{CO}_2} = 0.019$                          |
| $Y_{\text{O}_2} = 6 \times 10^{-4}$  | $Y_{(\text{WO}_3)_{n=1-3}} = 1-3.5 \times 10^{-4}$ | $Y_{\text{O}_2} = 3.6 \times 10^{-4}$  | $Y_{(\text{WO}_3)_{n=1-3}} = 1-4.2 \times 10^{-4}$ |

Further understanding of coupling and competitive reaction mechanisms will be needed in the near future to develop accurate models and mechanisms for the chemical erosion of rocket nozzles.

Assuming local thermodynamic equilibrium due to fast, high-temperature kinetics, estimates are made of the species present within the boundary layer of the tungsten nozzle. This is done by assuming a large portion of an equilibrium mixture to be crystallographic tungsten, as illustrated by the large quantity remaining in the equilibrium mixture (Table 3). The certainties of these results are limited not only by the accuracy of available thermodynamic data, but also by the number of known and characterized species available. The thermodynamic database used was the standard package provided with CEA, with several additional species and data included: namely, solid and gas phases of tungstic acid  $[\text{WO}_2(\text{OH})_2]$  [37] and tungsten hexacarbonyl  $[\text{W}(\text{CO})_6]$  [38], as well as solid phase ditungsten carbide ( $\text{W}_2\text{C}$ ) [38]. The calculations indicated  $\text{WO}_2(\text{OH})_2$  and  $\text{WO}_2\text{Cl}_2$  as the primary tungsten containing products. Tungsten trioxide ( $\text{WO}_3$ ) and its polymers are predicted to occur in greater quantities than  $\text{WO}_2$ . Assuming that in a simple  $\text{W}-\text{O}_2$  (or  $\text{W}-\text{CO}_2$ ) system the primary species formed is  $(\text{WO}_3)_n$ , this result provides a simple explanation and prediction of high-temperature tungsten oxidation rates while complicating overall mechanisms. The addition of  $\text{Cl}_2$  in the presence of  $\text{O}_2$  increases the stoichiometric coefficient (i.e.,  $\text{W}/\text{O}$  ratio) by forming the  $\text{WO}_2\text{Cl}_2$ , in turn increasing the tungsten oxidation or corrosion rate. Applying this methodology to the addition of hydrogen into an  $\text{O}_2$  system, forming  $\text{WO}_2(\text{OH})_2$  (i.e., reducing the stoichiometric coefficient), it is expected that oxidation rates would be reduced. Because chlorine and hydrogen are not present in the reaction systems of this study,  $\text{WO}_3$  or its dimer or trimer is assumed to be the primary product species when  $\text{O}_2$  and  $\text{CO}_2$  are the only oxidizing species. Although tungsten dioxide ( $\text{WO}_2$ ) is not a dominant equilibrium species, it may be a significant percentage of desorbed tungsten oxide, as indicated by the mass-spectrometric studies referenced.

#### IV. Conclusions

The heterogeneous reaction rates of bulk tungsten have been studied in the presence of oxygen, carbon dioxide, and carbon monoxide at high temperatures. Oxygen is a more efficient oxidizer with faster kinetics than  $\text{CO}_2$ , although both are found to oxidize tungsten at high rates, forming volatile oxide species and creating a linear mass loss of the bulk material at constant pressure and temperature conditions. The  $\text{W}-\text{O}_2$  and  $\text{W}-\text{CO}_2$  oxidation systems may be described using a single Arrhenius rate expression over the range of temperatures and pressures considered. The activation energy of the  $\text{CO}_2$  reaction is nearly 3 times larger than the  $\text{O}_2$  reaction (64 kcal/mol vs 23.5 kcal/mol). Computational and simplified theories indicate that the least energetically favorable reactions are surface oxide combination or desorption reactions. The pressure exponent of the  $\text{CO}_2$  reaction is found to be 0.6 versus 0.89 for the  $\text{O}_2$  reaction. Carbon monoxide does not oxidize tungsten to a volatile oxide; however, when added to a constant  $\text{CO}_2$  concentration mixture the overall oxidation rates are reduced significantly, providing further evidence of the importance in understanding detailed heterogeneous reaction mechanisms of single-, as well as multicomponent systems in order to model nozzle erosion rates. Simplified analysis of the reaction kinetics of  $\text{CO}_2$ ,  $\text{CO}$ , and  $\text{O}_2$  indicates that nozzle recession rates may be appreciably affected through small manipulations of propellant formulations without sacrificing propellant performance. This implies that rocket motor performance may be affected by small perturbations in propellant formulation due to changes in nozzle erosion rates.

#### Acknowledgments

The authors gratefully acknowledge financial support from the Office of Naval Research (ONR) under a MURI grant no. N00014-04-1-0683. The support and encouragement provided by Judah Goldwasser and Cliff Bedford is gratefully acknowledged. Additionally we would like to thank Dennis S. Fox of NASA

Glenn Research Center for his help in the development and design process of the TGA, and Larry Rothrock of Photran, LLC, for his help in the construction and procurement of sapphire hangers.

#### References

- [1] Opeka, M. M., "Thermodynamic-Based Materials Selection for Corrosion-Resistant Performance in High-Temperature Missile Propulsion Systems. Part 1. Consideration of Condensed Phase Equilibria," *Proceedings of Electrochemical Society*, Vol. 2004-16, 2004, pp. 253-267.
- [2] Acharya, R., and Kuo, K. K., "Graphite Rocket Nozzle Erosion Rate Reduction by Boundary-Layer Control Using Ablative Materials," *45th AIAA Aerospace Sciences Meeting and Exhibit*, AIAA, Reston, VA, 2007.
- [3] Evans, B., Kuo, K. K., Ferrara, P. J., Moore, J. D., Kutzler, P., and Boyd, E., "Nozzle Throat Erosion Characterization Study Using a Solid-Propellant Rocket Motor Simulator," *43rd AIAA/ASME/SAE/ASEE Joint Propulsion Conference & Exhibit*, AIAA, Reston, VA, 2007.
- [4] Liggett, N. D., and Menon, S., "Time-Dependent Nozzle Erosion Process in a Solid Propellant Rocket Motor," *43rd AIAA/ASME/SAE/ASEE Joint Propulsion Conference & Exhibit*, AIAA, Reston, VA, 2007.
- [5] Thakre, P., and Yang, V., "Chemical Erosion of Refractory Metal Nozzle Inserts in Solid-Propellant Rocket Motors," *46th AIAA Aerospace Sciences Meeting and Exhibit*, AIAA, Reston, VA, 2008.
- [6] Bartlett, E. P., "Thermal Protection of Rocket-Motor Structures," *Aerospace Engineering*, Vol. 22, No. 1, 1963, pp. 86-99.
- [7] Wong, E. Y., "Solid Rocket Nozzle Design Summary," *AIAA 4th Propulsion Joint Specialist Conference*, AIAA, New York, 1968.
- [8] Heath, G. A., and Thackray, R. W., "Chemical Erosion of Graphite Rocket Nozzles," *Journal of the British Interplanetary Society*, Vol. 22, No. 6, 1969, pp. 402-410.
- [9] De Morton, M. E., "Erosion in Rocket Motor Nozzles," *Wear*, Vol. 41, 1977, pp. 223-231.  
doi:10.1016/0043-1648(77)90003-5
- [10] Baur, J. P., Bridges, D. W., and Fassell, W. M., "High Pressure Oxidation of Metals—Tungsten in Oxygen," *Journal of the Electrochemical Society*, Vol. 103, No. 5, 1956, pp. 266-272.  
doi:10.1149/1.2430309
- [11] Gulbransen, E. A., and Andrew, K. F., "Kinetics of Oxidation of Pure Tungsten from 500 C to 1300 C," *Journal of the Electrochemical Society*, Vol. 107, No. 7, 1960, pp. 619-628.  
doi:10.1149/1.2427787
- [12] Perkins, R. A., and Crooks, D. D., "Low-Pressure, High-Temperature Oxidation of Tungsten," *Journal of Metals*, Vol. 13, No. 7, 1961, pp. 490-493.
- [13] Bartlett, R. W., "Tungsten Oxidation at High Temperatures," *Transactions of the Metallurgical Society of AIME*, Vol. 230, Aug. 1964, pp. 1097-1103.
- [14] Gulbransen, E. A., Andrew, K. F., and Brassart, F. A., "Kinetics of Oxidation of Pure Tungsten, 1150 C-1615 C," *Journal of the Electrochemical Society*, Vol. 111, No. 1, 1964, pp. 103-109.  
doi:10.1149/1.2426043
- [15] Walsh, P. N., Quets, J. M., and Graff, R. A., "Kinetics of the Oxygen-Tungsten Reaction at High Temperatures," *Journal of Chemical Physics*, Vol. 46, No. 3, 1967, pp. 1144-1153.  
doi:10.1063/1.1840781
- [16] Walsh, P. N., Quets, J. M., Graff, R. A., and Ladd, I. R., "Kinetics of the Oxidation of Tungsten by  $\text{CO}_2$  at High Temperatures," *Journal of Chemical Physics*, Vol. 46, No. 9, 1967, pp. 3571-3601.
- [17] Harvey, F. J., "High Temperature Oxidation of Tungsten Wires in  $\text{CO}_2$ -Argon Mixtures," *Metallurgical Transactions*, Vol. 5, Jan. 1974, pp. 35-38.
- [18] Farber, M., "High-Temperature Reaction Rates of Several Metals with Hydrogen Chloride and Water Vapor," *Journal of the Electrochemical Society*, Vol. 106, No. 9, 1959, pp. 751-754.  
doi:10.1149/1.2427491
- [19] Kilpatrick, M., and Lott, S. K., "Reaction of Flowing Steam with Refractory Metals 3. Tungsten (1000-1700 C)," *Journal of the Electrochemical Society*, Vol. 113, No. 1, 1966, pp. 17-18.  
doi:10.1149/1.2423850
- [20] Unal, C., Bohl, W. R., and Pasamehmetoglu, K. O., "Modeling of Heat and Mass Transfer in Accelerator Targets During Postulated Accidents," *Nuclear Engineering and Design*, Vol. 196, 2000, pp. 185-200.  
doi:10.1016/S0029-5493(99)00297-6
- [21] Greene, G. A., and Finfrook, C. C., "Vaporization of Tungsten in



- Flowing Steam at High Temperatures," *Experimental Thermal and Fluid Science*, Vol. 25, 2001, pp. 87–99.  
doi:10.1016/S0894-1777(01)00063-2
- [22] Rosner, D. E., and Allendorf, H. D., "Kinetics of the Attack of High-Temperature Molybdenum and Tungsten by Atomic Oxygen," *Journal of the Electrochemical Society*, Vol. 114, No. 4, 1967, pp. 305–314.  
doi:10.1149/1.2426583
- [23] Farber, M., Darnell A. J., and Ehrenberg, D. M., "High Temperature Corrosion Rates of Several Metals with Nitric Oxide," *Journal of the Electrochemical Society*, Vol. 102, No. 8, 1955, pp. 446–453.  
doi:10.1149/1.2430122
- [24] Olcott, E. L., and Batchelor, J. D., "Failure Mechanisms in Dense Tungsten Alloy Rocket Nozzles," *Journal of Spacecraft and Rockets*, Vol. 1, No. 6, 1964, pp. 635–642.  
doi:10.2514/3.27714
- [25] Rosner, D. E., and Allendorf, H. D., "Ablation Rates in Mixtures of Reactive Gases," *AIAA Journal*, Vol. 5, No. 8, 1967, pp. 1489–1491.  
doi:10.2514/3.4225
- [26] Rosner, D. E., "Convective Diffusion as an Intruder in Kinetic Studies of Surface Catalyzed Reactions," *AIAA Journal*, Vol. 2, No. 4, 1964, pp. 593–610.  
doi:10.2514/3.2393
- [27] Sabourin, J. L., and Yetter, R. A., "High Temperature Oxidation of Tungsten and Its Role in Rocket Nozzle Erosion," *JANNAF Rocket Nozzle Technology Subcommittee Meeting*, 2007.
- [28] Harvey, F. J., "High Temperature Oxidation of Tungsten Wires in O<sub>2</sub>-Ar Mixtures," *Metallurgical Transactions*, Vol. 4, June 1973, pp. 1513–1517.
- [29] Kee, R. J., Rupley, F. M., Miller, J. A., Coltrin, M. E., Grcar, J. F., Meeks, E., Moffat, H. K., Lutz, A. E., Dixon-Lewis, G., Smooke, M. D., Warnatz, J., Evans, G. H., Larson, R. S., Mitchell, R. E., Petzold, L. R., Reynolds, W. C., Caracotsios, M., Stewart, W. E., Glarborg, P., Wang, C., Adigun, O., Houf, W. G., Chou, C. P., Miller, S. F., Ho, P., Young, P. D., and Young, D. J., CHEMKIN Ver. 4.0.2, Reaction Design, Inc., San Diego, CA, 2005.
- [30] McBride, B. J., and Gordon, S., Computer Program for Calculation of Complex Chemical Equilibrium Compositions and Applications, NASA, 1996.
- [31] Chen, H., Musaev, D. G., and Lin, M. C., "Adsorption and Dissociation of CO<sub>x</sub> (x = 1, 2) on W(111) Surface: A Computational Study," *Journal of Physical Chemistry C*, Vol. 112, No. 9, 2008, pp. 3341–3348.  
doi:10.1021/jp709575r
- [32] Chen, L., Sholl, D. S., and Johnson, J. K., "First Principles Study of Adsorption and Dissociation of CO on W(111)," *Journal of Physical Chemistry B*, Vol. 110, No. 3, 2006, pp. 1344–1349.  
doi:10.1021/jp055374z
- [33] Hwu, H. H., Polizzotti, B. D., and Chen, J. G., "Potential Application of Tungsten Carbides as Electrocatalysts. 2. Coadsorption of CO and H<sub>2</sub>O on Carbide-Modified W(111)," *Journal of Physical Chemistry B*, Vol. 105, No. 41, 2001, pp. 10045–10053.  
doi:10.1021/jp0116205
- [34] Berkowitz-Mattuck, J. B., Buchler, A., Engelke, J. L., and Goldstein, S. N., "Mass-Spectrometric Investigation of the Oxidation of Molybdenum and Tungsten," *Journal of Chemical Physics*, Vol. 39, No. 10, 1963, pp. 2722–2730.  
doi:10.1063/1.1734090
- [35] Schissel, P. O., and Trulson, O. C., "Mass-Spectrometric Study of the Oxidation of Tungsten," *Journal of Chemical Physics*, Vol. 43, No. 2, 1965, pp. 737–743.  
doi:10.1063/1.1696799
- [36] Azens, A., Kitenbergs, M., and Kanders, U., "Evaporation of Tungsten Oxides: A Mass-Spectrometric Study of the Vapor Contents," *Vacuum*, Vol. 46, No. 7, 1995, pp. 745–747.  
doi:10.1016/0042-207X(94)00074-3
- [37] *JANAF Thermochemical Tables*, edited by M. W. Chase, American Chemical Society, Washington, D.C., 1986.
- [38] *Thermochemical Properties of Inorganic Substances*, edited by O. Knacke, O. Kubaschewski, and K. Hesselmann, Springer-Verlag, Berlin, 1991.

C. Avedisian  
Associate Editor